

Research outputs 2022 to 2026

6-1-2023

Saudi Arabian basalt/CO₂/brine wettability: Implications for CO₂ geo-storage

Muhammad Ali
Edith Cowan University

Nurudeen Yekeen
Edith Cowan University

Amer Alanazi

Alireza Keshavarz
Edith Cowan University

Stefan Iglauer
Edith Cowan University

See next page for additional authors

Follow this and additional works at: <https://ro.ecu.edu.au/ecuworks2022-2026>

 Part of the Chemical Engineering Commons

[10.1016/j.est.2023.106921](https://doi.org/10.1016/j.est.2023.106921)

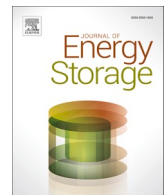
Ali, M., Yekeen, N., Alanazi, A., Keshavarz, A., Iglauer, S., Finkbeiner, T., & Hoteit, H. (2023). Saudi Arabian basalt/CO₂/brine wettability: Implications for CO₂ geo-storage. *Journal of Energy Storage*, 62, Article 106921.

<https://doi.org/10.1016/j.est.2023.106921>

This Journal Article is posted at Research Online.
<https://ro.ecu.edu.au/ecuworks2022-2026/2168>

Authors

Muhammad Ali, Nurudeen Yekeen, Amer Alanazi, Alireza Keshavarz, Stefan Iglauer, Thomas Finkbeiner, and Hussein Hoteit



Research papers

Saudi Arabian basalt/CO₂/brine wettability: Implications for CO₂ geo-storage



Muhammad Ali ^{a,b,*}, Nurudeen Yeeken ^b, Amer Alanazi ^a, Alireza Keshavarz ^b, Stefan Iglaue ^b, Thomas Finkbeiner ^a, Hussein Hoteit ^{a,*}

^a Physical Science and Engineering Division, King Abdullah University of Science and Technology (KAUST), Thuwal 23955, Saudi Arabia

^b School of Engineering, Edith Cowan University, Joondalup 6027, Western Australia, Australia

ARTICLE INFO

Keywords:

Carbon capture and geo-storage
Saudi Arabian basalt
CO₂ wettability
Organic acid

ABSTRACT

The geological sequestration of carbon dioxide, including mineralization in basaltic formations, has been identified as a promising method of attaining a low-carbon economy. However, successful CO₂ storage depends on both the CO₂ wettability of the basaltic rocks and the basalt rock-fluid interfacial interactions. The contact angles of brine/CO₂ systems for Western Australian (WA) and Iceland basalts have been recently reported in the literature. However, contact angle datasets for evaluating the CO₂ wettability of Saudi Arabian (SA) basalt have not been previously reported. Moreover, there is limited information on the impact of organic acids on the wettability of the basalt/CO₂/brine system. In the present study, the contact angles of supercritical CO₂/brine systems on SA basalt are measured at temperatures of 298 and 323 K, and at various pressures of 0.1–20 MPa in the absence and presence of organic acid (10⁻² mol/L stearic acid). Various analytical methods are used to characterize the SA basalt surface, and the wetting behavior of the SA basalt is compared with that of the WA and Iceland basalts. The quantity of CO₂ that can be safely trapped underneath the SA basalt (in terms of CO₂ column height) is then computed from the experimental data. At the highest tested temperature and pressure (20 MPa and 323 K), the pure SA basalt is found to remain strongly water-wet, with advancing (θ_a) and receding (θ_r) contact angles of 46.7° and 43.2°, respectively, whereas the Iceland basalt becomes moderately water-wet ($\theta_a = 85.1^\circ$ and $\theta_r = 81.8^\circ$), and the WA basalt becomes CO₂-wet ($\theta_a = 103.6^\circ$ and $\theta_r = 96.1^\circ$). However, the organic-aged SA basalt attains a CO₂-wet state ($\theta_a = 106.8^\circ$ and $\theta_r = 95.2^\circ$). In addition, the CO₂ column height of the pure SA basalt is higher than that reported for the WA and Iceland basalts. Further, at 323 K, the CO₂ column height decreases from 835 m at 5 MPa to –957 m at 20 MPa. These results suggest that there could be both freer plumb and lateral movement of CO₂ into the SA basalt in the presence of organic acid, thus resulting in lower residual and mineral trapping capacities, and fewer eventual leakages of CO₂, across the geological formation.

1. Introduction

The injection of carbon dioxide (CO₂) into geological formations is a promising process for decreasing global warming and achieving a low-CO₂ global economy [1–5]. Saudi Arabia is a major hydrocarbon-producing nation with several existing infrastructures and transportation pipelines for natural gas storage, and these could be used for large-scale CO₂ storage in depleted hydrocarbon reservoirs, saline aquifers, and salt caverns [6–8]. In addition, sedimentary formations such as shales, tight sandstone or carbonates and igneous rocks (such as basalts) have been recently identified as promising formations that

could be explored for CO₂ storage [9–16].

Basalts are dark-colored, fine-grained, igneous rocks comprising mainly pyroxene, plagioclase, and other minerals such as olivine. They are more abundant and readily available than shales [14,15]. Indeed, the Cenozoic volcanic rocks in Saudi Arabia are among the main zones of alkali olivine basalt in the world, covering almost 90,000 km² [17,18]. The principal mechanism of CO₂ storage in reactive rocks such as basalt has been identified as carbon mineralization, and studies have demonstrated that basalt may be suitable for CO₂ storage via this mechanism, or via residual trapping when the basalt formation is topped by a caprock [19–21]. Moreover, basalt is universally distributed with good

* Corresponding authors at: Physical Science and Engineering Division, King Abdullah University of Science and Technology (KAUST), Thuwal 23955, Saudi Arabia.

E-mail addresses: Muhammad.ali.2@kaust.edu.sa (M. Ali), [H. Hoteit](mailto:Hussein.hoteit@kaust.edu.sa).

vesicular texture, significant thickness, and favorable mineral composition [12,15,22–25]. Hence, the injection of CO₂ into volcanic (igneous) rocks such as basalt can swiftly initiate carbon mineralization and mineral trapping, in contrast to the poor trapping performance of the silica minerals in sedimentary formations [9,10]. Surprisingly, pilot project trials conducted in Washington State (USA) [24] and Iceland [12] revealed that most of the CO₂ injected into basalt rock was mineralized in less than two years.

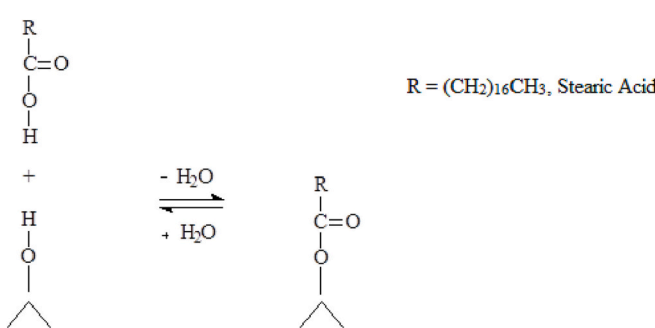
Some researchers have attempted to estimate the entire volume of basalt geological sites accessible for CO₂ storage. For example, McGrail et al. used a volumetric technique under the assumption that the average porosity and thickness are 15 % and 10 m, respectively, and that the hydrostatic pressure is 10 MPa, to estimate the CO₂ storage capacity of Colombia River basalt as 100 Gt [23]. Meanwhile, Anthonsen et al. [26] used the same assumptions to estimate the CO₂ storage capacity of Iceland basalt to be 60 Gt. More recently, the subsurface CO₂ storage potentials of basaltic rocks from Saudi Arabia have been assessed by researchers. For instance, Oelkers et al. [14] found that mineralization reactions provide the Jizan basalts of southwest Saudi Arabia with a CO₂ storage potential of 1.4–10.2 Gt, which would be adequate for storing the CO₂ that is projected to be emitted from Jizan Economic City over the coming 100–140 years. The results of Monte Carlo simulation predictions further suggested that mafic igneous rocks in the Jizan area have a total CO₂ mineralization capacity of almost 4.2 Gt, which is sufficient to store all of the projected CO₂ emissions from the local industrial facilities for the next 400 years.

A few researchers have also studied the wettability of basalt/CO₂/brine systems. For instance, Al-Yaseri et al. [9] found that originally water-wet Western Australian (WA) basalt became moderately-to-fully CO₂-wet when the pressure was increased beyond 15 MPa at 323 K. Meanwhile, Iglaue et al. [10] reported that Iceland basalt is strongly hydrophilic below 500 m depth, but becomes moderately wettable at 900 m. However, to the best of the present authors' knowledge, there is no reported research on the wetting behavior of Saudi Arabian (SA) basalt for the assessment of CO₂ storage feasibility in this region. Hence, in the present study, the contact angles of supercritical CO₂/brine systems on Saudi Arabian (SA) basalt substrates are measured at temperatures 298 and 323 K and various pressures of 0.1–20 MPa in the absence and presence of organic acid (10^{−2} mol/L stearic acid) to mimic the actual reservoir conditions [27–33]. The CO₂ wetting behaviors of the SA basalts under reservoir conditions (higher pressures and higher temperatures) are then compared with those of WA and Iceland basalts. The experimental data are then used to determine the quantity of CO₂ (in terms of column height) that could be safely trapped underneath the SA basalt. The results of this research are expected to assist in evaluating and optimizing the geological storage of CO₂ in Saudi Arabian basaltic regions.

2. Materials and methods

2.1. Materials

The solid substrates for the basalt-CO₂-brine wettability measurements were acquired from Harrat Rahat near the Red Sea coast of Western Saudi Arabia [34]. The basaltic rock thin sections were then prepared and polished for cleaning, aging with stearic acid, and contact angle measurement. The CO₂ gas (purity = 99.999 %) was obtained from BOC Australia, and the brine solution (0.3 M NaCl) was prepared using 99.999 mol% pure NaCl (electrical conductivity = 0.02 mS/cm) obtained from ChemLab, Australia. For substrate surface cleaning, 99.999 % ultra-pure nitrogen was obtained from BOC Australia. The stearic acid solution (10^{−2} mol/L; 99.95 % purity, Sigma Aldrich, Australia) was prepared by dissolving in n-decane. All other solvents, including acetone, toluene, hydrochloric acid, and methanol (99.999 mol%) were obtained from Rowe Scientific.



Scheme 1. Organic acid chemisorption on the solid basalt substrate (\wedge represents the solid basalt) [30,31].

2.2. Characterization of the pure and organic-aged SA basalts

The detailed composition and bulk mineralogy of the SA basalt were determined via X-ray diffraction (XRD; Bruker Model D8 Discover) [35], and the quantitative bulk mineralogy was obtained via the Rietveld method. The average pore throat radius and surface area were obtained via the Brunauer–Emmett–Teller (BET) method. The elemental compositions and morphologies of the pure and organic-aged SA basalt substrates were determined via field emission scanning electron microscopy (FESEM with energy dispersive spectroscopy (EDS; Oxford Instruments). The total organic content (TOC) was measured via pyrolysis using a Rock-Eval 6 apparatus (Vinci Technologies, Nanterre, France) [36,37]. The levels of stearic acid adsorption and functional groups on the organic-aged SA basalt substrates were examined by Fourier transform infrared (FTIR) spectroscopy (Spectrum Two, PerkinElmer) in the range of 400–4000 cm^{−1} [38].

For the surface roughness measurements, the SA basalt substrate was cut in suitable dimensions of 20 × 20 × 5 mm (length x width x height) using a high-speed diamond blade, and then polished with abrasive paper (sizes 400 and 1200). The surface roughness was then measured via atomic force microscopy (AFM; Nano-surf, Flex-Axiom, and Controller C3000). For the contact angle measurements, the SA basalt substrates were first cleaned with deionized water to remove any surface dust and minimize the impact of substrate surface contamination. Water droplets and any other surface impurities were then removed by ultra-pure nitrogen gas, followed by air plasma for 20 min (Diemer Yocto) to ensure that any organic contamination was removed.

2.3. Substrate aging

The SA basalt was aged in 10^{−2} mol/L stearic acid solution to simulate realistic subsurface storage conditions, where the surface of the rock is in contact with organic molecules (organic contamination) for several years [39–42]. The substrates were then aged by dipping in 2 wt % NaCl solution (pH equilibrated at 4 pKa) for 0.5 h to ionize the basalt surface [27,43]. The pH was controlled using aqueous droplets of diluted hydrochloric acid (37.5 wt%) in NaCl solution. This procedure promotes organic acid adsorption on the basalt surface [27,32,43]. The thin brine film on the basalt surface was removed using ultra-pure nitrogen. Afterward, the HCl/brine-ionized basalt substrates were immersed in an n-decane/organic acid solution (10^{−2} mol/L) in a ratio of 1:5 (i.e., 1 g of basalt and 5 g of n-decane/organic acid solution) for 7 days to imitate the exposure of basalt to formation waters. The organic acid esterification on the hydroxyl groups of the basalt surface leads to covalent bonding and increases the surface hydrophobicity of the basalt, as indicated in Scheme 1 [44,45].

2.4. Contact angle measurement

In a given CO₂/brine/mineral system, the wettability alteration

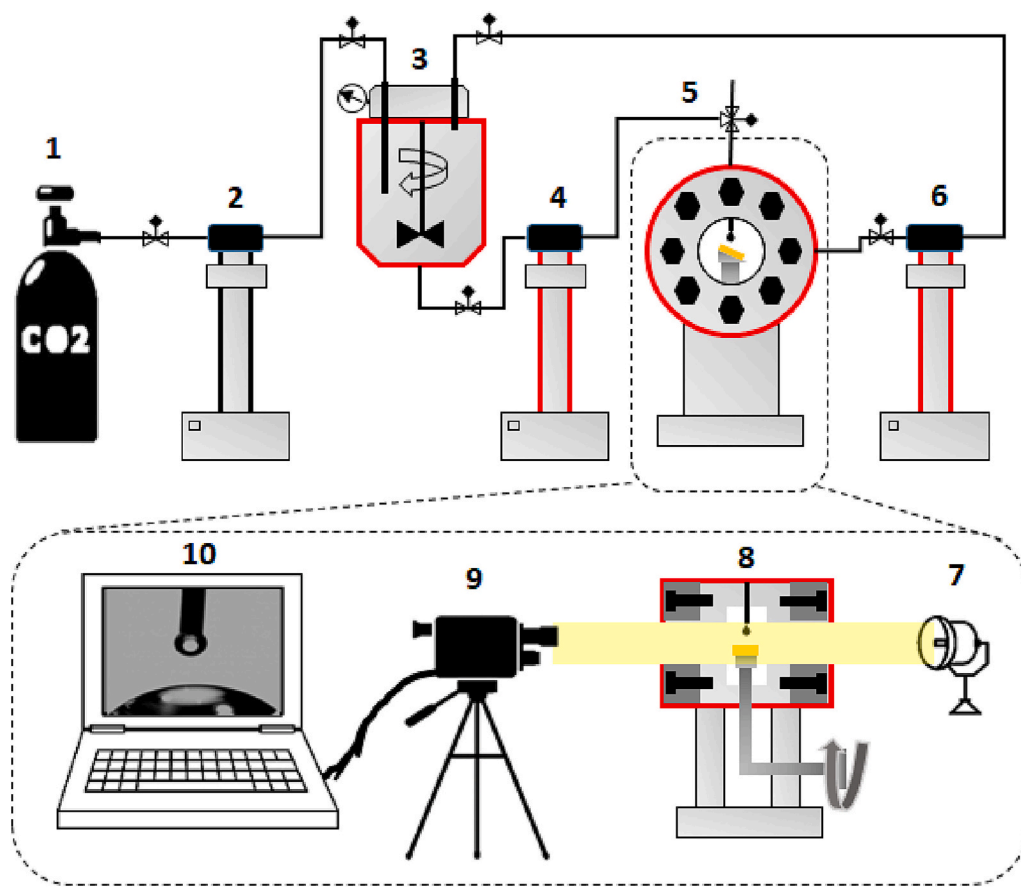


Fig. 1. A schematic diagram of the contact angle measurement system for use under high pressure and high temperature (HPHT) conditions: (1) CO₂ supply via pressurized bottle; (2) HPHT precision syringe pump for CO₂ injection into the mixing reactor (ISCO Company, USA); (3) dissolution of CO₂ in brine via HPHT mixing reactor (Parr Company); (4) HPHT precision syringe pump for live brine injection; (5) front view of the tilted-plate HPHT interfacial contact angle (IFT) cell; (6) HPHT precision syringe pump for CO₂ injection into the IFT cell; (7) brightness adjustment via light projection; (8) side view of the tilted plate HPHT IFT cell; (9) video recording; (10) interpretation of the results.

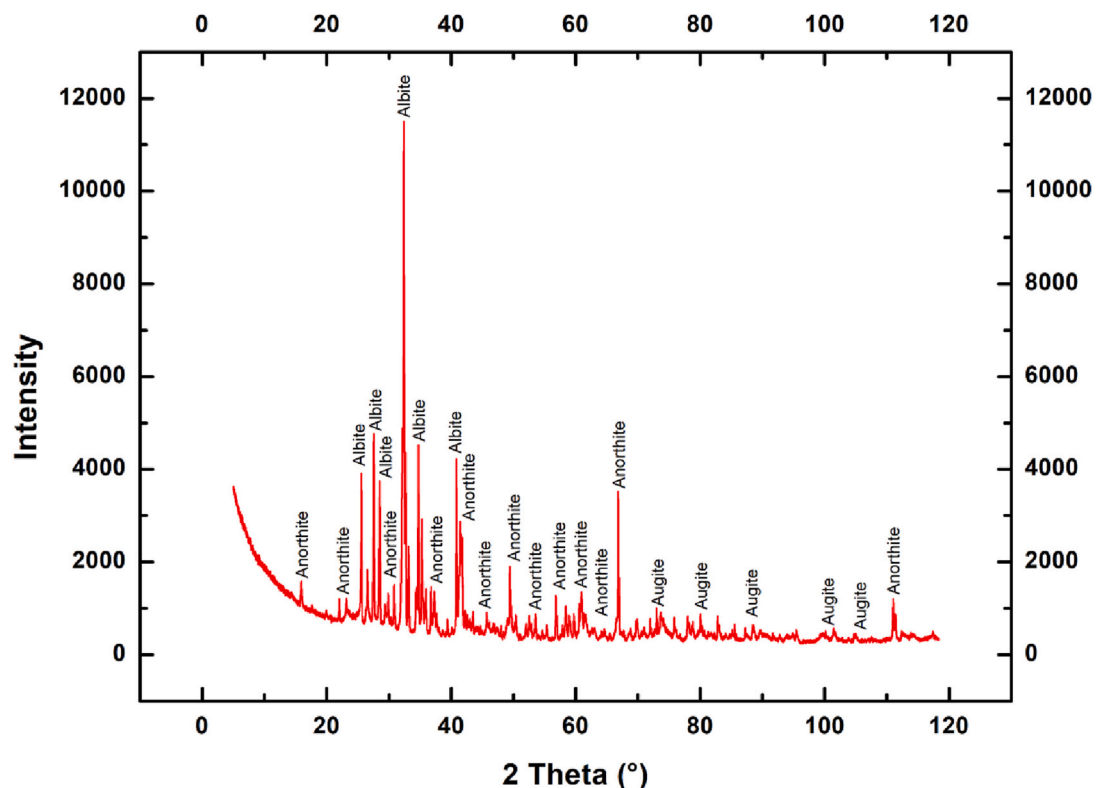


Fig. 2. The XRD pattern of the SA basalt.

Table 1

The quantitative composition of the SA basalt from the XRD analysis.

Mineral phase	Composition (wt%)
Anorthite ($\text{CaAl}_2\text{Si}_2\text{O}_8$)	51
Augite [$(\text{Ca}, \text{Na})(\text{Mg}, \text{Fe}, \text{Al}, \text{Ti})(\text{Si}, \text{Al})_2\text{O}_6$]	16
Albite ($\text{NaAlSi}_3\text{O}_8$)	33

behavior is widely comprehended via contact angle measurements [46]. In this test, the tilted plate technique is used to determine the leading (advancing) and trailing (receding) tangent angles, designated θ_a and θ_r , respectively, that can be achieved at the typical reservoir temperatures and pressures [47]. In the present work, the brine (0.3 M NaCl) was first equilibrated with CO_2 and the SA basalt substrates under the prerequisite subsurface conditions in a mixing reactor (Parr Instruments) operating at 1200 rpm to minimize the effects of mass-transfer due to basalt surface-brine interactions [48]. The advancing and receding contact angles were then measured via the tilted plate goniometric technique at typical geo-storage temperatures and pressures (298 and 323 K; 0.1–20 MPa). The system used in the present work is shown schematically in Fig. 1. Thus, the basalt substrate was placed in the viewing cell, and then ultra-pure CO_2 was injected as the surrounding fluid. A droplet of the equilibrated brine (5.5 μL) was then dispensed onto the basalt surface, and the θ_a and θ_r were measured before droplet movement. The procedure was video recorded using a high-performance video camera (Fujinon CCTV lens: HF35HA-1B; 1:1.6/35 mm, frame rate = 71 fps; pixel size = 7.4 μm ; Basler scA 640–70 fm) followed by image extraction using the ImageJ software. The standard deviation of

all contact angles was $\pm 3^\circ$ based on repeated measurements. A similar methodology was used for contact angle measurements in previous studies by the present authors [27,29,33,49].

3. Results and discussion

3.1. Characterization of the SA basalt samples

The XRD peaks and patterns of the SA basalt samples are presented in Fig. 2, and the quantitative bulk mineralogy is presented in Table 1. The results of BET analysis indicate an average pore throat radius of 2.4 nm and a BET surface area of $9.6656 \text{ m}^2/\text{g}$.

The AFM images in Fig. 3 indicate a root mean square (RMS) surface roughness of 210 nm, thus suggesting that the SA basalt samples have smooth surface profiles. Hence, the impact of surface roughness upon the contact angle measurement will be insignificant, as the RMS value is less than 1 μm [50–52].

The FESEM micrographs of the pure and aged basalt samples are presented in Fig. 4a and b, respectively. Here, it is clear that organic acid adsorption has created a monolayer on the basalt surface. This is confirmed by the EDS results in Table 2, where the carbon content is seen to increase from 11.7 wt% for the pure SA basalt to 19.04 wt% for the organic-aged SA basalt. This increase in carbon content will result in an increased hydrophobicity of the aged basalt surface [29,31,53,54]. Further, the results in Table 2 indicate that the SA basalt samples have a diverse mineral composition, with C, O, Na, Mg, Al, Si, Ca, Fe, and Ba being the major components.

The adsorption of stearic acid on the organic-aged SA basalt is

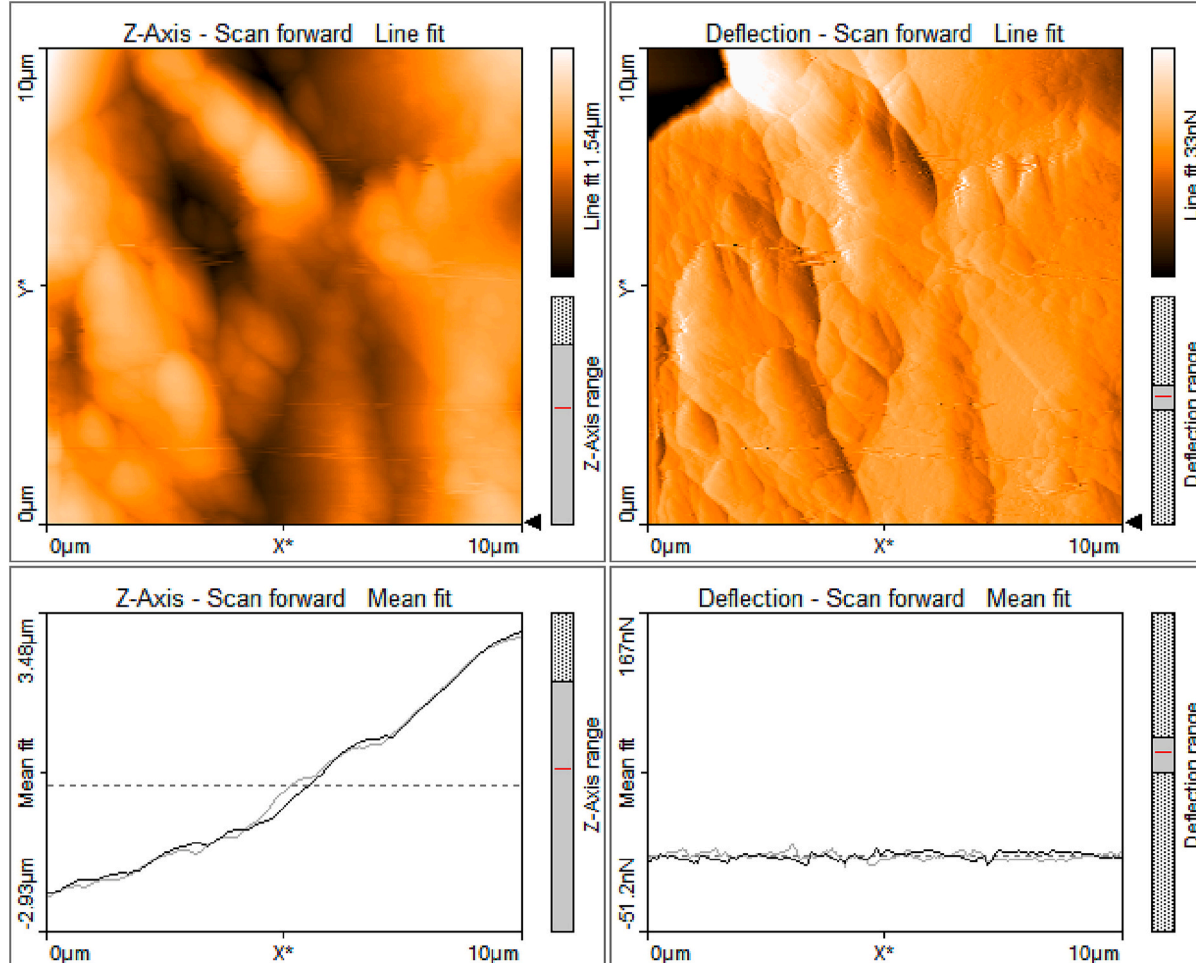


Fig. 3. The AFM images and corresponding surface roughness profiles of the SA basalt.

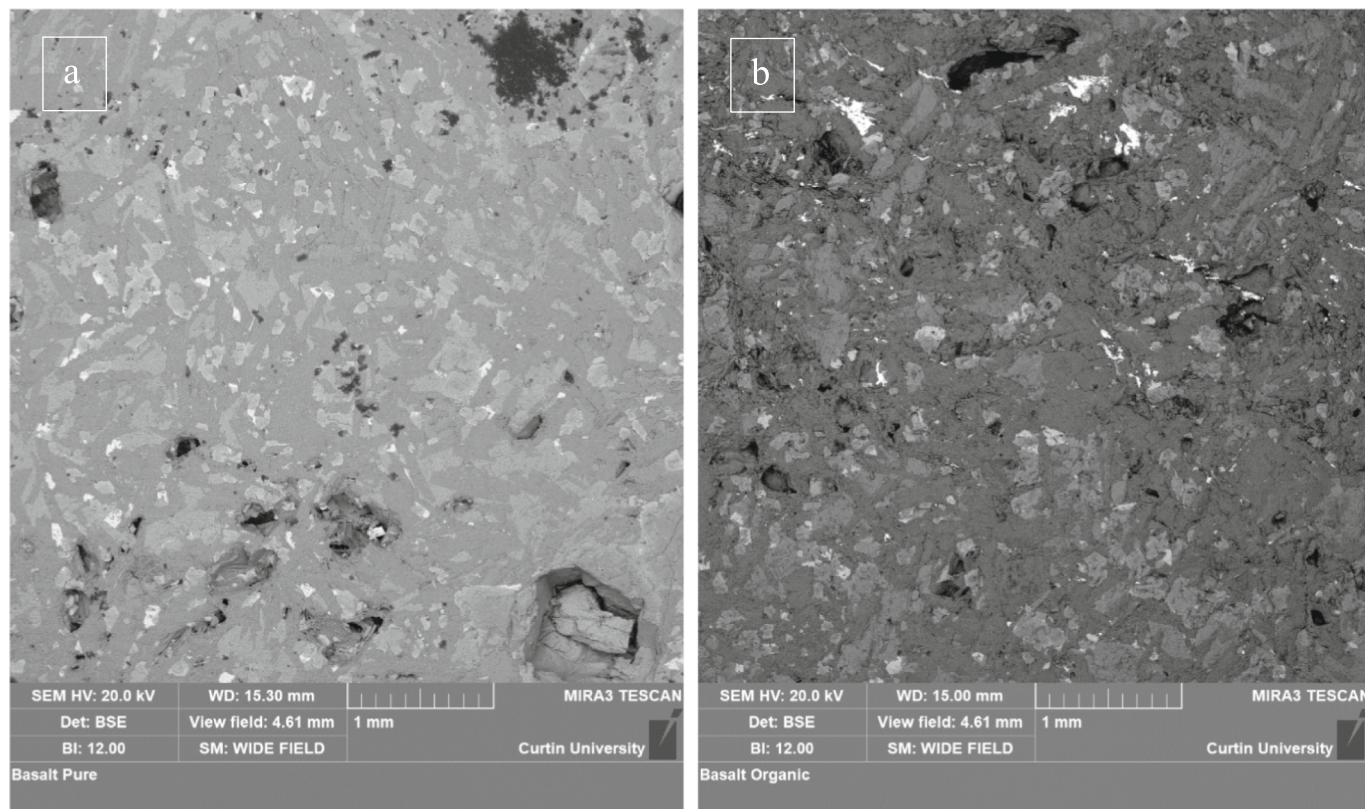


Fig. 4. The SEM images of (a) the pure SA basalt, and (b) the organic-aged SA basalt.

Table 2

The elemental compositions of the pure and organic-aged SA basalt samples.

Element	Pure SA basalt (wt%)	Organic-aged SA basalt (wt %)	Standard label
C	11.70	19.04	C Vit
O	35.74	32.70	N/A
Na	2.42	2.07	Albite
Mg	2.22	2.08	MgO
Al	8.44	8.64	Al ₂ O ₃
Si	16.30	15.63	SiO ₂
S	–	0.92	FeS ₂
Cl	0.07	–	NaCl
K	0.42	0.47	KBr
Ca	12.71	5.32	Wollastonite
Ti	1.56	0.57	Ti
Mn	0.12	0.13	Mn
Fe	8.28	7.61	Fe
Ba	–	4.84	BaF ₂
Total:	100.00	100.00	–

confirmed by the TOC measurements in Fig. 5. Thus, the TOC of the pure SA basalt is 400 ppm, while that of the organic-aged SA basalt is 700 ppm due to the adsorption of organic acid molecules on the basalt surface [55,56].

The extent of stearic acid adsorption and functional groups on the SA basalt substrates are further revealed by the FTIR spectra in Fig. 6. Here, the FTIR spectrum of the pure SA basalt exhibits characteristic peaks at 1600–2000 and 800 cm⁻¹ due to the Si—OH and —OH vibrations, respectively, on the basalt surface. By contrast, while the stretching peak at 2000 cm⁻¹ is also observed in the stearic-acid aged SA basalt, additional sharp adsorption bands are observed between 2750 and 3000 cm⁻¹ due to the symmetric and asymmetric C—H stretching vibrations of CH₂ [57,58], along with peaks at 1250–1500 cm⁻¹ due to the Si—CH₂ bending vibrations, and bands between 750 and 1000 cm⁻¹ due to the

Si—O—C and Si—O stretching vibrations. These results suggest that the surface of the organic-aged SA basalt has been rendered hydrophobic due to the chemical reactions/interactions between the hydroxyl groups of the organic acid and those of the basalt surface (Scheme 1) [9,29,59].

3.2. The CO₂/brine wettability of various basalts under typical reservoir conditions

The rock-fluid interaction and wetting characteristics are crucial parameters that control the spreading of the gas (CO₂ in the present case) through the geological formation [60–62]. In addition, these factors regulate the storage capacities [63–65] and fluid flow dynamics throughout the porous media [46,63,66], along with the gas injection rates [46,67], gas withdrawal rates [68–70], and safety of gas entrapment [49,71–73]. In this context, the receding contact angle (θ_r) is used for the condition in which CO₂ is injected, and the brine is displaced; when θ_r exceeds 90°, it may affect the structural entrapment of the gas [74]. Meanwhile, the advancing contact angle (θ_a) describes the situation in which brine is re-imbibed and entraps the CO₂ gas into clusters, thereby causing residual trapping; when θ_a exceeds 50°, this may affect the primary drainage [69,75–77]. Furthermore, each natural geo-storage formation has an inherent organic presence, which may significantly affect the storage capacity [39,40,42,102]. Therefore, to elucidate these various effects, the measured contact angles (θ_a and θ_r) of the pure SA basalt are compared with those of other basaltic formations and the organic-aged SA basalt substrates in the following subsections.

3.2.1. The CO₂/brine wettability of pure Saudi Arabian (SA), Western Australian (WA), and Iceland basalts at various temperatures and pressures

The SA basalt/CO₂/brine, WA basalt/CO₂/brine, and Iceland basalt/CO₂/brine contact angles under geo-storage conditions are compared in Fig. 7. Here, both the θ_a and θ_r are seen to increase with the increase in temperature and pressure for all samples, in agreement with the results of previous research [9,10,78]. This suggests that the intermolecular

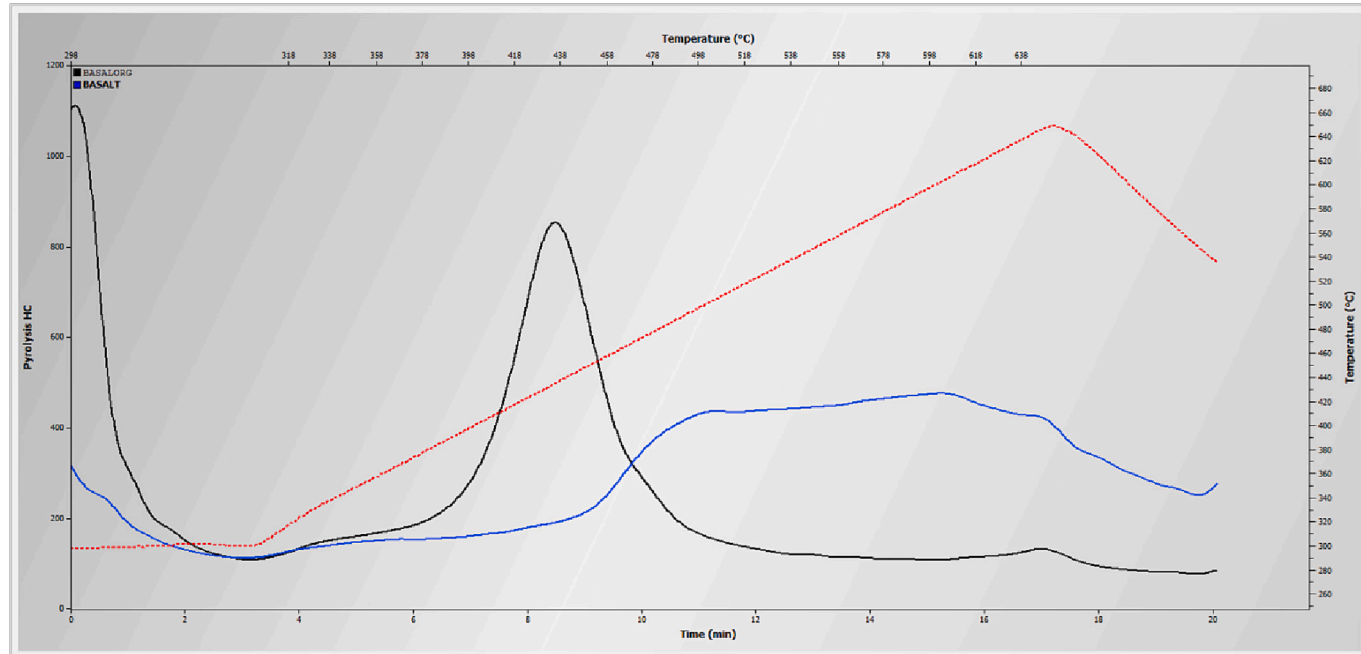


Fig. 5. The TOC profiles of the pure (blue) and organic-aged (black) SA basalt, along with the temperature profile (red). (For interpretation of the references to color in this figure legend, the reader is referred to the web version of this article.)

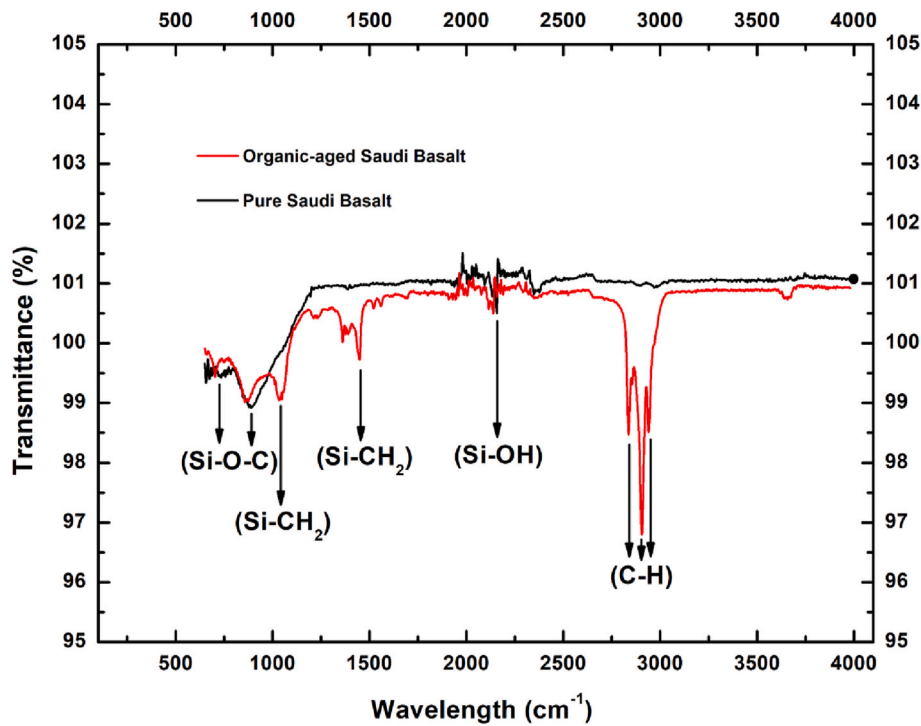


Fig. 6. The FTIR spectra of the pure and organic-aged SA basalt.

interactions between the basalt and CO₂ are increased due to the impacts of temperature and pressure upon the CO₂ density. Thus, at the highest investigated pressure (20 MPa), the SA basalt remains water wet at both 298 and 323 K. The WA and Iceland basalts are each found to be more hydrophobic than the SA basalt under similar thermo-physical conditions. For instance, at 323 K and 20 MPa, the WA basalt becomes CO₂-wet ($\theta_a = 103.6^\circ$ and $\theta_r = 96.1^\circ$), whereas the SA basalt remains water-wet ($\theta_a = 46.7^\circ$ and $\theta_r = 43.2^\circ$). Meanwhile, under similar conditions of 313.15 K and 17 MPa, the Iceland basalt becomes intermediately water-

wet ($\theta_a = 85.1^\circ$ and $\theta_r = 81.8^\circ$).

These results can be attributed to the differences in the mineralogical compositions of the SA, WA, and Iceland basalts. The most copious phases in these basalts are the sodium alumina-silicate (NaAlSi₃O₈) and calcium alumina-silicate (CaAl₂Si₂O₈) plagioclases, comprising 33 and 51 wt%, respectively, in the SA Basalt (Table 1). Meanwhile, previous studies have indicated total plagioclase compositions of 59 and 80 wt% for the Iceland and WA basalts, respectively [9,10]. Previous studies have also shown that plagioclase exhibits a hydrophobic (dispersive)

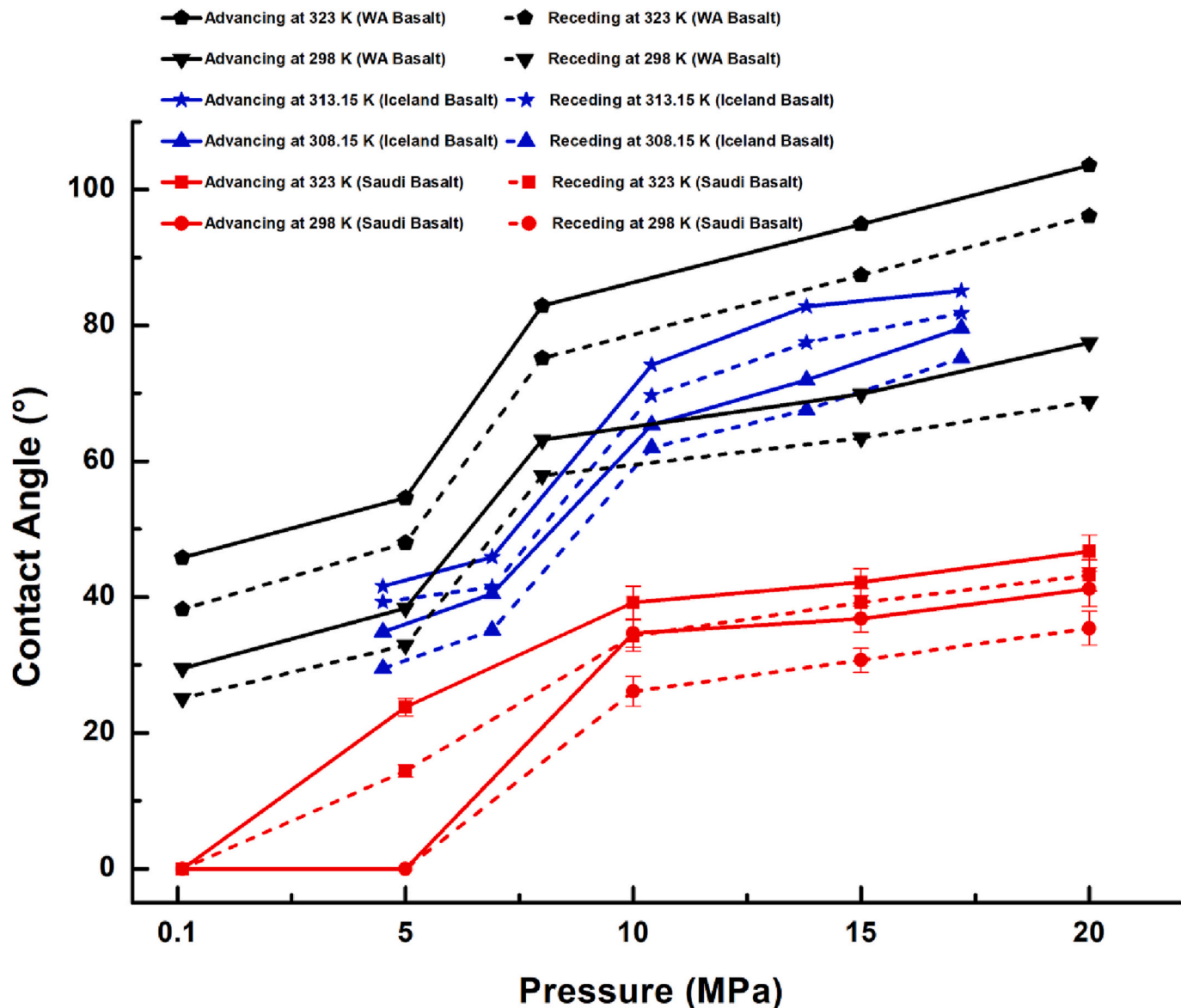


Fig. 7. The CO₂/brine contact angles of the SA, WA, and Iceland basalts at various temperatures and pressures.

interaction, having a low interfacial tension with water, and that the higher advancing and receding contacts of the WA basalt/CO₂/brine system are due to the higher plagioclase content compared to the Iceland basalt [9,10,78]. Similarly, it is inferred that the elevated θ_a and θ_r values in the WA and Iceland basalts are due to their higher plagioclase contents compared to that of the SA basalt in the present study. In brief, the higher the plagioclase content, the higher the rock hydrophobicity. Thus, the WA and Iceland basalts are expected to show stronger CO₂-wetting responses than the SA basalt under realistic geo-storage conditions. These results further suggest that the mineralization reaction between carbon dioxide and basalt will significantly affect the basalt wettability, because the CO₂/basalt and water/basalt interfacial areas will vary according to the wetting conditions. Because the WA and Iceland basalt become hydrophobic under the CO₂-wet and intermediately water-wet states, fewer dissolution and precipitation reactions are anticipated due to a significant decrease in the basalt/water interfacial areas. The resulting substantial reduction in the capillary and structural trapping capacities of these basalts will facilitate vertical movement of CO₂ in the reservoir, thus leading to leakages of CO₂ across the basalt formation [9,10,78].

3.2.2. The comparison of CO₂ wettability of the pure and organic-aged SA basalt

Previous studies have suggested that the CO₂ wettability of the SA basalt will be significantly impacted by the organic acid contamination inherent in geological formations, and that the contact angles steadily increase in the presence of organic acid, and CO₂ pressure [29,39,40]. Indeed, the results in Fig. 8 indicate that a minute concentration (10⁻² mol/L) of stearic acid substantially impacts the CO₂ wettability of the aged SA basalt compared to pure SA basalt. For instance, the wettability of the SA basalt at 323 K and 5 MPa is altered from a strongly water-wet state ($\theta_a = 23.8^\circ$ and $\theta_r = 14.4^\circ$) for the pure SA basalt to an intermediately water-wet condition ($\theta_a = 87.3^\circ$ and $\theta_r = 79.1^\circ$) for the aged SA basalt. Further, when the pressure is increased to 20 MPa at the same temperature, the organic-aged SA basalt attains a CO₂-wet state, with $\theta_a = 106.8^\circ$ and $\theta_r = 95.2^\circ$, thus confirming that the presence of organic acid can significantly affect the CO₂ trapping capacities of the basaltic formations. These results are attributed to the covalent chemical reaction between the hydroxyl group of the basalt substrate and the hydroxyl group of the organic acid (Scheme 1) [29,49,79].

Notably, the actual basaltic formations used for the geological storage of CO₂ may contain even higher concentrations of organic acid than

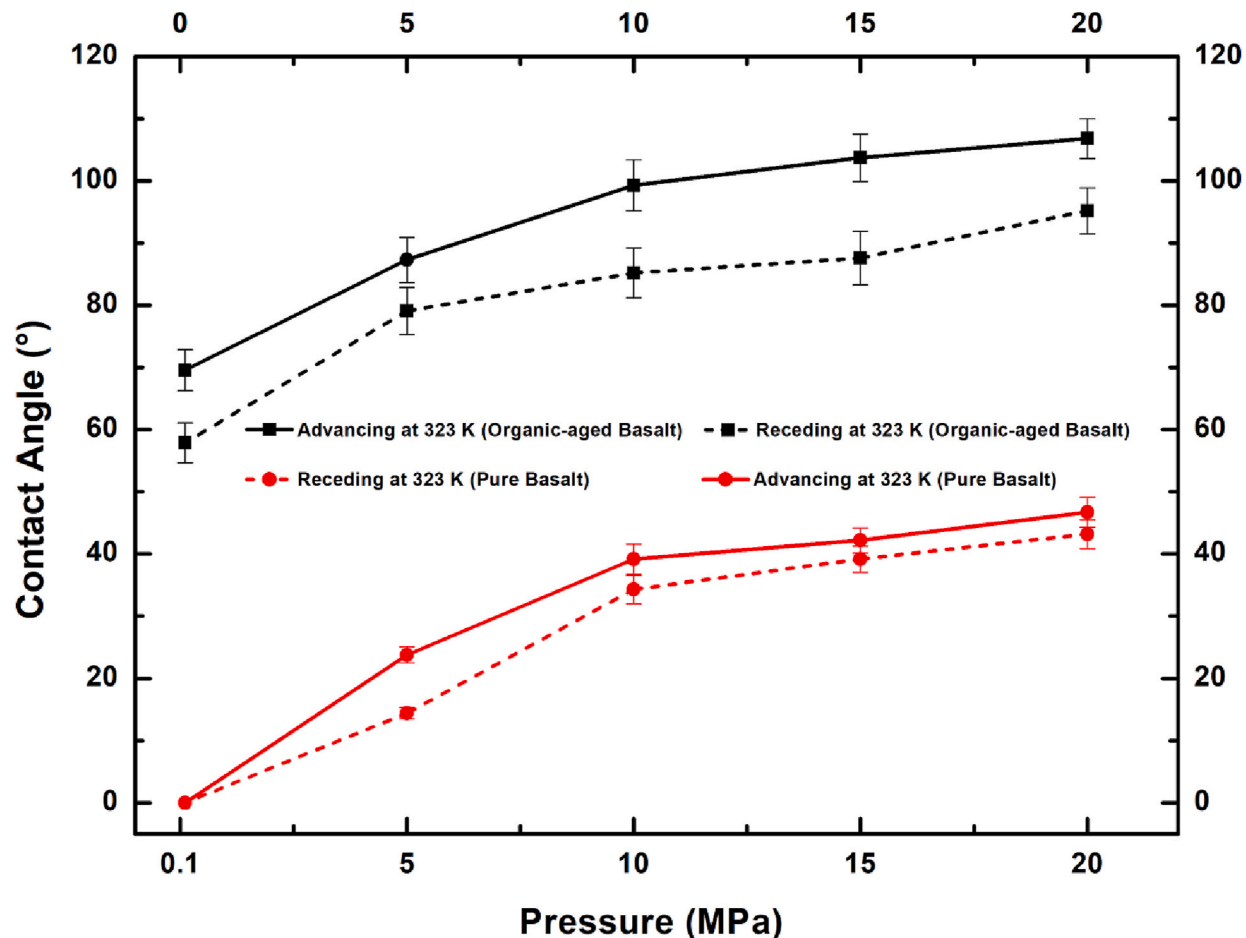


Fig. 8. The CO₂ wettability of the pure (red) and organic-aged (black) SA basalt at various pressures. (For interpretation of the references to color in this figure legend, the reader is referred to the web version of this article.)

the 10⁻² mol/L used in the present study. Consequently, the attendant impact of organic contamination upon the trapping of CO₂ in basaltic formations could be more than expected. Both the θ_a and θ_r values are higher at higher pressure due to the stronger interactions between the CO₂ gas molecules and the SA basalt substrates [80]. The high-pressure contact angle results obtained herein are congruous with the previously-published literature for other rock types, where the increasing pressure also increased the CO₂ density and, hence, the intermolecular interactions between the rock surfaces and CO₂ molecules [11,33,51,81–84].

In addition, as the stearic-acid- aged SA basalt attains intermediate and CO₂-wet states at higher pressures, more CO₂ molecules will occupy the pores, thereby decreasing the pore occupancy of the residual brine. This process could increase the proportion of CO₂ molecules interacting with or contacting the surface of the SA basalt, thereby resulting in a rapid upward migration of CO₂ [63,64,85,86]. Thus, it can be inferred that the presence of organic acid in geo-storage formations will decrease the CO₂ geo-storage capacity, ultimately resulting in specifically low containment safety of CO₂ in the basaltic formations. This applies when the CO₂ escapes from the aqueous phase into the gaseous phase in basaltic rocks [74,76]. The results of previous studies have shown that an increasing CO₂ wettability of the basaltic rock could alter the interfacial area/reactions between the basalt and brine, as well as the rate of mineralization, depending on the capillary pressure and pore morphology [9,10,59,78].

3.2.3. The CO₂ column heights of the SA basalt

To assess the sealing potential of the SA basalt at a typical geo-

storage temperature (323 K) and various pressures (5–20 MPa), the column height of CO₂ that could be securely trapped within the SA basalt is computed using Eq. (1) [87]:

$$h_{\max} = \frac{2\gamma \cos \theta}{\Delta \rho g r} \quad (1)$$

where h_{\max} is the CO₂ column height, γ is the CO₂/brine interfacial contact angle (IFT), θ is the receding contact angle of the CO₂/brine system on SA basalt, g is the gravitational constant (9.81 m/s²), r is the average pore-throat radius of the SA basalt (2.4 nm, from the BET analysis), and $\Delta \rho$ is the CO₂/brine density difference obtained from the literature [88–90]. Here, the CO₂ is assumed to be in the gaseous phase, the basalt formation is assumed to have several layers acting as caprock, and the IFT values are obtained from the literature [91,92]. The column height is computed using the receding contact angle dataset because it relates to the entry of CO₂ into the caprock and the displacement of resident brine by the CO₂ [2].

The results of this calculation are presented in Fig. 9. Here, the CO₂ column height of the pure SA basalt is calculated to be 4275 m at 5 MPa, but decreases to 3949 m at 10 MPa. The CO₂ column height then increases to 6354 m at 15 MPa, and to 7699 m at 20 MPa (green line, Fig. 9). The reduction in CO₂ column height in going from 5 to 10 MPa can be attributed to the drastic decreases in both the CO₂/brine density difference (from 930.55 to 655.8 kg/m³) and the IFT (from 48.35 mN/m to 36.9 mN/m). These values continue to decrease as the pressure increases to 15 MPa, where $\Delta \rho = 345.5$ kg/m³, and $\gamma = 33.35$ mN/m. However, the CO₂ tends towards supercritical at 10 MPa, but remains in the liquid form up to 20 MPa, which could contribute to the decrease in column height between 5 and 10 MPa, as well as explaining the

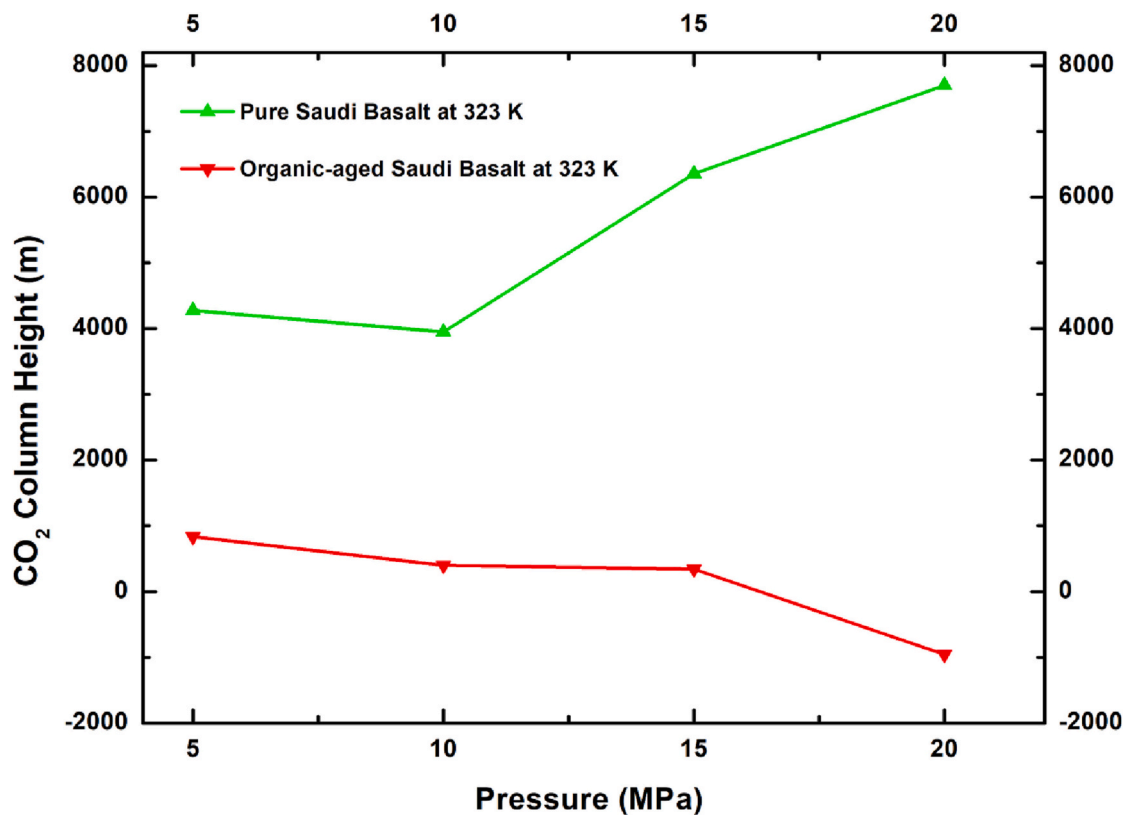


Fig. 9. The CO₂ column heights of the pure and organic-aged SA basalts as a function of pressure.

subsequent increase in column height with the further increase in pressure up to 20 MPa, in spite of the continued decreases in $\Delta\rho$ and γ . Moreover, the results in Fig. 9 indicate that the height of the CO₂ column that can be trapped underneath the pure SA basalt is higher (due to lower contact angles) than that under the WA basalt and Iceland basalt (due to higher contact angles, compare Fig. 7). Further, this can also be attributed to the lower average pore-throat radius of the SA basalt (2.4 nm) compared to that of the Iceland and WA basalts (29 nm each), which would lead to stronger capillary forces during CO₂ storage in the SA basalt.

By contrast, the CO₂ column height of the organic-aged SA basalt (red line, Fig. 9) is seen to decrease with increasing pressure, thereby attaining negative values at 20 MPa. In detail, the CO₂ column height decreases from 835 m at 5 MPa to ~-957 m at 20 MPa as the SA basalt becomes CO₂-wet ($\theta_r = 95.2^\circ$). These results clearly demonstrate the significant impact of organic acid contamination upon CO₂ storage in the SA basalt, thereby suggesting a high CO₂ leakage risk due to decreasing capillary/residual trapping of the CO₂ as the injection depth increases in organic acid-contaminated SA basalt. Hence, to keep CO₂ immobilized in such basalt, it is essential to keep the CO₂ injection depth range as narrow as possible in order to avoid exceeding the pressure at which the SA basalt will retain its water-wet condition. In the case of CO₂ storage in organic-aged SA basalt, the effect of the organic acid is expected to predominate over that of the capillary pressure, and the ramifications should be considered before the injection of CO₂ in such formations.

4. Conclusions

The sequestration of CO₂ in a geological formation is a promising approach to minimizing the impact of anthropogenic CO₂ gas emissions and preventing global warming [2,3,93]. However, the storage potential of a given geological formation depends on its wetting characteristics, cap-rock, and interactions with the brine/CO₂ system [60,84,94–97]. In

turn, the rock wettability can be affected by the geological storage temperature and pressure, and by the inherent presence of organic acids in the storage formation [29,98–101]. Hence, the wettability of Saudi Arabian (SA) basalt/CO₂/brine system was examined herein, along with the impact of an organic acid (stearic acid) upon the wetting behavior during CO₂ storage. To this end, the advancing (θ_a) and receding (θ_r) contact angles of the pure and organic-aged CO₂/brine systems were measured under typical reservoir conditions, and were compared with those of Western Australian (WA) and Iceland basalts. The results indicated that the contact angles increase with increasing temperature and pressure, in agreement with the majority of previous studies on basalt substrates [9,10,78]. Further, the contact angles of the pure SA basalt/CO₂/brine system were lower than those of the organic-aged SA basalt/CO₂/brine system, and the former system remained strongly water-wet under all tested conditions. Meanwhile, the organic-aged SA basalt attained the CO₂-wet state ($\theta_a = 106.8^\circ$ and $\theta_r = 95.2^\circ$) at 20 MPa and 323 K. In the case of CO₂ escaping from the aqueous phase to the gaseous phase, assuming the absence of any fractures, the height of the gaseous CO₂ column that could be trapped underneath the pure SA basalt rocks was shown to be higher than that of the WA and Iceland basalts. These results were attributed to the differences in rock mineralogy (plagioclase content) and the low average pore-throat radius of the SA basalt (2.4 nm). Meanwhile, the CO₂ column height of the organic-aged SA basalt decreased from 835 m at 5 MPa to ~-957 m at 20 MPa due to a drastic increase in CO₂-wetting behavior. This suggests that reservoir models should account for the effect of organics in order to accurately calculate the CO₂ geo-storage potential, and the ramifications should be considered for enhanced containment security.

CRediT authorship contribution statement

Muhammad Ali: Conceptualization, Methodology, Validation, Investigation, Data curation, Writing – original draft, Writing – review & editing. **Nurudeen Yeeken:** Visualization, Writing – review & editing.

Amer Alanazi: Validation, Formal analysis. **Alireza Keshavarz:** Data curation, Methodology. **Stefan Iglauer:** Software, Validation. **Thomas Finkbeiner:** Validation, Writing – review & editing. **Hussein Hoteit:** Resources, Writing – review & editing, Project administration, Supervision.

Declaration of competing interest

The authors declare that they have no known competing financial interests or personal relationships that could have appeared to influence the work reported in this paper.

Data availability

All the data is already presented in the article.

Acknowledgment

This publication is supported by the King Abdullah University of Science and Technology (KAUST) Research Funding Office under Award No. 4357.

References

- [1] N. Yekeen, E. Padmanabhan, A. Thenesh, L. Sevoo, A. Kamalarasan, L. Kanesen, O.A. Okunade, Wettability of rock/CO₂/brine systems: a critical review of influencing parameters and recent advances, *J. Ind. Eng. Chem.* 88 (2020) 1–28.
- [2] M. Ali, N.K. Jha, N. Pal, A. Keshavarz, H. Hoteit, M. Sarmadivaleh, Recent advances in carbon dioxide geological storage, experimental procedures, influencing parameters, and future outlook, *Earth Sci. Rev.* 225 (2022), 103895.
- [3] F.J.F.M. Blunt Jr., F.M. Orr, Carbon dioxide in enhanced oil recovery, *Energy Convers. Manag.* 34 (1993) 9–11.
- [4] F.M. Orr, Onshore geologic storage of CO₂, *Science* 325 (5948) (2009) 1656–1658.
- [5] A. Hamieh, F. Rowaihy, M. Al-Juaied, A.N. Abo-Khatwa, A.M. Afifi, H. Hoteit, Quantification and analysis of CO₂ footprint from industrial facilities in Saudi Arabia, *Energy Convers. Manag.* X 16 (2022), 100299.
- [6] I. Tili, Renewable energy in Saudi Arabia: current status and future potentials, *Environ. Dev. Sustain.* 17 (4) (2015) 859–886.
- [7] Y.A. Amran, Y.M. Amran, R. Alyousef, H. Alabduljabbar, Renewable and sustainable energy production in Saudi Arabia according to Saudi Vision 2030: current status and future prospects, *J. Clean. Prod.* 247 (2020), 119602.
- [8] R. Weijermars, D. Al-Shehri, Regulation of oil and gas reserves reporting in Saudi Arabia: review and recommendations, *J. Pet. Sci. Eng.* 210 (2022), 109806.
- [9] A. Al-Yaseri, M. Ali, M. Ali, R. Taheri, D. Wolff-Boenisch, Western Australia basalt-CO₂-brine wettability at geo-storage conditions, *J. Colloid Interface Sci.* 603 (2021) 165–171.
- [10] S. Iglauer, A.Z. Al-Yaseri, D. Wolff-Boenisch, Basalt-CO₂-brine wettability at storage conditions in basaltic formations, *Int. J. Greenh. Gas Control.* 102 (2020), 103148.
- [11] H. Abdulelah, A. Al-Yaseri, M. Ali, A. Giwelli, B.M. Negash, M. Sarmadivaleh, CO₂/Basalt's interfacial tension and wettability directly from gas density: implications for carbon geo-sequestration, *J. Pet. Sci. Eng.* 204 (2021), 108683.
- [12] S.R. Gislason, D. Wolff-Boenisch, A. Stefansson, E.H. Oelkers, E. Gunnlaugsson, H. Sigurdardottir, B. Sigfusson, W.S. Broecker, J.M. Matter, M. Stute, Mineral sequestration of carbon dioxide in basalt: a pre-injection overview of the CarbFix project, *Int. J. Greenh. Gas Control.* 4 (3) (2010) 537–545.
- [13] M. Hosseini, M. Ali, J. Fahimpoor, A. Keshavarz, S. Iglauer, Basalt-H₂-brine wettability at geo-storage conditions: implication for hydrogen storage in basaltic formations, *J. Energy Storage* 52 (2022), 104745.
- [14] E.H. Oelkers, S. Arkadakskiy, A.M. Afifi, H. Hoteit, M. Richards, J. Fedorik, A. Delaunay, J.E. Torres, Z.T. Ahmed, N. Kunnummal, The subsurface carbonation potential of basaltic rocks from the Jizan region of Southwest Saudi Arabia, *Int. J. Greenh. Gas Control.* 120 (2022), 103772.
- [15] J.E.A. Torres, The Potential for CO₂ Disposal in Western Saudi Arabia, The Jizan Group Basalts, 2020.
- [16] A.A. Mahesar, M. Ali, A.M. Shar, K.R. Memon, U.S. Mohanty, H. Akhondzadeh, A. H. Tunio, S. Iglauer, A. Keshavarz, Effect of cryogenic liquid nitrogen on the morphological and petrophysical characteristics of tight gas sandstone rocks from kirthar fold belt, Indus Basin, Pakistan, *Energy Fuel* 34 (11) (2020) 14548–14559.
- [17] R.G. Coleman, R. Gregory, G.F. Brown, Cenozoic Volcanic Rocks of Saudi Arabia, US Department of the Interior, Geological Survey, 1983.
- [18] S. Arkadakskiy, E. Oelkers, A. Afifi, H. Hoteit, S. Gislason, N. Kunnummal, Z. Ahmed, The potential for sequestering CO₂ in basalts along the Red Sea Coast of Saudi Arabia, in: AGU Fall Meeting Abstracts, 2020 pp. GC111-05.
- [19] C. Cao, H. Liu, Z. Hou, F. Mehmood, J. Liao, W. Feng, A review of CO₂ storage in view of safety and cost-effectiveness, *Energies* 13 (3) (2020) 600.
- [20] P. Kelemen, S.M. Benson, H. Pilorgé, P. Psarras, J. Wilcox, An overview of the status and challenges of CO₂ storage in minerals and geological formations, *Front. Clim.* 1 (2019) 9.
- [21] M. Kang, J.H. Kim, K.-O. Kim, S. Cheong, Y.J. Shinn, Assessment of CO₂ storage capacity for basalt caprock-sandstone reservoir system in the northern East China Sea, in: EGU General Assembly Conference Abstracts, 2018, p. 5772.
- [22] G. Yododzinski, T. Naumann, E.I. Smith, T. Bradshaw, J.D. Walker, Evolution of a mafic volcanic field in the central Great Basin, south central Nevada, *J. Geophys. Res. Solid Earth* 101 (B8) (1996) 17425–17445.
- [23] B.P. McGrail, H.T. Schaef, A.M. Ho, Y.J. Chien, J.J. Dooley, C.L. Davidson, Potential for carbon dioxide sequestration in flood basalts, *J. Geophys. Res. Solid Earth* 111 (B12) (2006).
- [24] B.P. McGrail, H.T. Schaef, F.A. Spane, J.A. Horner, A.T. Owen, J.B. Cliff, O. Qafoku, C.J. Thompson, E.C. Sullivan, Wallula basalt pilot demonstration project: post-injection results and conclusions, *Energy Procedia* 114 (2017) 5783–5790.
- [25] H. Wu, R.S. Jayne, R.J. Bodnar, R.M. Polleyea, Simulation of CO₂ mineral trapping and permeability alteration in fractured basalt: implications for geologic carbon sequestration in mafic reservoirs, *Int. J. Greenh. Gas Control.* 109 (2021), 103383.
- [26] K. Anthonsen, P. Aagaard, P. Bergmo, M. Erlström, J. Fareide, S. Gislason, G. Mortensen, S. Snæbjörnsdóttir, CO₂ storage potential in the Nordic region, *Energy Procedia* 37 (2013) 5080–5092.
- [27] M. Ali, Effect of Organic Surface Concentration on CO₂-wettability of Reservoir Rock, Curtin University, 2018.
- [28] M. Ali, Effect of Organics and Nanoparticles on CO₂-wettability of Reservoir Rock; Implications for CO₂ Geo-storage, Curtin University, 2021.
- [29] M. Ali, A. Aftab, Z.-U.-A. Arain, A. Al-Yaseri, H. Roshan, A. Saeedi, S. Iglauer, M. Sarmadivaleh, Influence of organic acid concentration on wettability alteration of cap-rock: implications for CO₂ trapping/storage, *ACS Appl. Mater. Interfaces* 12 (35) (2020) 39850–39858.
- [30] M. Ali, S. Al-Anssari, M. Arif, A. Barifcany, M. Sarmadivaleh, L. Stalker, M. Lebedev, S. Iglauer, Organic acid concentration thresholds for ageing of carbonate minerals: implications for CO₂ trapping/storage, *J. Colloid Interface Sci.* 534 (2019) 88–94.
- [31] M. Ali, M. Arif, M.F. Sahito, S. Al-Anssari, A. Keshavarz, A. Barifcany, L. Stalker, M. Sarmadivaleh, S. Iglauer, CO₂-wettability of sandstones exposed to traces of organic acids: implications for CO₂ geo-storage, *Int. J. Greenh. Gas Control.* 83 (2019) 61–68.
- [32] M. Ali, N. Yekeen, M. Ali, M. Hosseini, N. Pal, A. Keshavarz, S. Iglauer, H. Hoteit, Effects of various solvents on adsorption of organics for porous and nonporous quartz/CO₂: implications for CO₂ geo-storage, *Energy Fuel* 36 (18) (2022) 11089–11099.
- [33] M. Ali, N. Yekeen, N. Pal, A. Keshavarz, S. Iglauer, H. Hoteit, Influence of organic molecules on wetting characteristics of mica/H₂/brine systems: implications for hydrogen structural trapping capacities, *J. Colloid Interface Sci.* 608 (2022) 1739–1749.
- [34] M.R. Moufti, K. Németh, Harrat Rahat: the geoheritage value of the youngest long-lived volcanic field in the Kingdom of Saudi Arabia, in: *Geoheritage of Volcanic Harrats in Saudi Arabia*, Springer, 2016, pp. 33–120.
- [35] P. Eskelinen, X-ray diffraction study of TiO₂ thin films on mica, *J. Solid State Chem.* 100 (2) (1992) 356–362.
- [36] M. Alshakhs, M.R. Rezaee, A new method to estimate total organic carbon (TOC) content, an example from Goldwyer Shale Formation, the Canning Basin, *Open Pet. Eng. J.* 10 (2017) 118–133.
- [37] H. Yu, R. Rezaee, Z. Wang, T. Han, Y. Zhang, M. Arif, L. Johnson, A new method for TOC estimation in tight shale gas reservoirs, *Int. J. Coal Geol.* 179 (2017) 269–277.
- [38] F.U.R. Awan, A. Keshavarz, H. Akhondzadeh, S.F. Al-Anssari, A.Z. Al-Yaseri, A. Nosrati, M. Ali, S. Iglauer, Stable dispersion of coal fines during hydraulic fracturing flowback in coal seam gas reservoirs—an experimental study, *Energy Fuel* 34 (5) (2020) 5566–5577.
- [39] P.D. Lundegard, Y.K. Kharaka, Distribution and Occurrence of Organic Acids in Subsurface Waters, *Organic Acids in Geological Processes*, Springer, 1994, pp. 40–69.
- [40] D.M. Akob, I.M. Cozzarelli, D.S. Dunlap, E.L. Rowan, M.M. Lorah, Organic and inorganic composition and microbiology of produced waters from Pennsylvania shale gas wells, *Appl. Geochem.* 60 (2015) 116–125.
- [41] H.J. Ulrich, W. Stumm, B. Cosovic, Adsorption of aliphatic fatty acids on aquatic interfaces. Comparison between two model surfaces: the mercury electrode and 8-Al₂O₃ colloids, *Environ. Sci. Technol.* 22 (1) (1988) 37–41.
- [42] B. Caballero, L.C. Trugo, P.M. Finglas, *Encyclopedia of Food Sciences and Nutrition*, Academic, 2003.
- [43] M. Ali, N. Yekeen, N. Pal, A. Keshavarz, S. Iglauer, H. Hoteit, Influence of pressure, temperature and organic surface concentration on hydrogen wettability of caprock; implications for hydrogen geo-storage, *Energy Rep.* 7 (2021) 5988–5996.
- [44] S. Al-Anssari, M. Arif, S. Wang, A. Barifcany, M. Lebedev, S. Iglauer, Wettability of nanofluid-modified oil-wet calcite at reservoir conditions, *Fuel* 211 (2018) 405–414.
- [45] S. Al-Anssari, A. Barifcany, S. Wang, L. Maxim, S. Iglauer, Wettability alteration of oil-wet carbonate by silica nanofluid, *J. Colloid Interface Sci.* 461 (2016) 435–442.
- [46] S. Iglauer, CO₂-water-rock wettability: variability, influencing factors, and implications for CO₂ geostorage, *Acc. Chem. Res.* 50 (5) (2017) 1134–1142.

- [47] L.M. Lander, L.M. Siewierski, W.J. Brittain, E.A. Vogler, A systematic comparison of contact angle methods, *Langmuir* 9 (8) (1993) 2237–2239.
- [48] R. El-Maghrary, C. Pentland, S. Iglauder, M. Blunt, A fast method to equilibrate carbon dioxide with brine at high pressure and elevated temperature including solubility measurements, *J. Supercrit. Fluids* 62 (2012) 55–59.
- [49] M. Ali, A. Aftab, F.U.R. Awan, H. Akhondzadeh, A. Keshavarz, A. Saeedi, S. Iglauder, M. Sarmadivaleh, CO₂-wettability reversal of cap-rock by alumina nanofluid: implications for CO₂ geo-storage, *Fuel Process. Technol.* 214 (2021), 106722.
- [50] A. Marmur, Soft contact: measurement and interpretation of contact angles, *Soft Matter* 2 (1) (2006) 12–17.
- [51] A.Z. Al-Yaseri, M. Lebedev, A. Barifcani, S. Iglauder, Receding and advancing (CO₂ + brine+ quartz) contact angles as a function of pressure, temperature, surface roughness, salt type and salinity, *J. Chem. Thermodyn.* 93 (2016) 416–423.
- [52] M. Hosseini, J. Fahimpour, M. Ali, A. Keshavarz, S. Iglauder, Hydrogen wettability of carbonate formations: implications for hydrogen geo-storage, *J. Colloid Interface Sci.* 614 (2022) 256–266.
- [53] M. Ali, N.K. Jha, A. Al-Yaseri, Y. Zhang, S. Iglauder, M. Sarmadivaleh, Hydrogen wettability of quartz substrates exposed to organic acids; implications for hydrogen geo-storage in sandstone reservoirs, *J. Pet. Sci. Eng.* 207 (2021), 109081.
- [54] A. Al-Yaseri, N. Yekeen, M. Ali, N. Pal, A. Verma, H. Abdulelah, H. Hoteit, M. Sarmadivaleh, Effect of organic acids on CO₂-rock and water-rock interfacial tension: implications for CO₂ geo-storage, *J. Pet. Sci. Eng.* 214 (2022), 110480.
- [55] H.R. Abid, N. Yekeen, A. Al-Yaseri, A. Keshavarz, S. Iglauder, The impact of humic acid on hydrogen adsorptive capacity of eagle ford shale: implications for underground hydrogen storage, *J. Energy Storage* 55 (2022), 105615.
- [56] M. Ali, F.U.R. Awan, M. Ali, A. Al-Yaseri, M. Arif, M. Sánchez-Román, A. Keshavarz, S. Iglauder, Effect of humic acid on CO₂-wettability in sandstone formation, *J. Colloid Interface Sci.* 588 (2021) 315–325.
- [57] S. Mahamuda, K. Swapna, M. Venkateswarlu, A.S. Rao, S. Shakya, G.V. Prakash, Spectral characterisation of Sm³⁺ ions doped oxy-fluoroborate glasses for visible orange luminescent applications, *J. Lumin.* 154 (2014) 410–424.
- [58] K. Swapna, S. Mahamuda, A.S. Rao, S. Shakya, T. Sasikala, D. Haranath, G. V. Prakash, Optical studies of Sm³⁺ ions doped zinc alumino bismuth borate glasses, *Spectrochim. Acta Mol. Biomol. Spectrosc.* 125 (2014) 53–60.
- [59] A. Al-Yaseri, N.K. Jha, On hydrogen wettability of basaltic rock, *J. Pet. Sci. Eng.* 200 (2021), 108387.
- [60] E.A. Al-Khdheewi, S. Vialle, A. Barifcani, M. Sarmadivaleh, S. Iglauder, Impact of reservoir wettability and heterogeneity on CO₂-plume migration and trapping capacity, *Int. J. Greenh. Gas Control* 58 (2017) 142–158.
- [61] E.A. Al-Khdheewi, S. Vialle, A. Barifcani, M. Sarmadivaleh, S. Iglauder, Influence of injection well configuration and rock wettability on CO₂ plume behaviour and CO₂ trapping capacity in heterogeneous reservoirs, *J. Nat. Gas Eng.* 43 (2017) 190–206.
- [62] S. Al-Anssari, Z.-U.-A. Arain, H.A. Shanshool, M. Ali, A. Keshavarz, S. Iglauder, M. Sarmadivaleh, Effect of nanoparticles on the interfacial tension of CO-oil system at high pressure and temperature: an experimental approach, in: SPE Asia Pacific Oil & Gas Conference and Exhibition, Society of Petroleum Engineers, 2020.
- [63] S. Iglauder, A.Z. Al-Yaseri, R. Rezaee, M. Lebedev, CO₂ wettability of caprocks: implications for structural storage capacity and containment security, *Geophys. Res. Lett.* 42 (21) (2015) 9279–9284.
- [64] S. Iglauder, C. Pentland, A. Busch, CO₂ wettability of seal and reservoir rocks and the implications for carbon geo-sequestration, *Water Resour. Res.* 51 (1) (2015) 729–774.
- [65] M. Arif, M. Lebedev, A. Barifcani, S. Iglauder, Influence of shale-total organic content on CO₂ geo-storage potential, *Geophys. Res. Lett.* 44 (17) (2017) 8769–8775.
- [66] M. Ali, N.U. Dahraj, S.A. Haider, Study of asphaltene precipitation during CO₂ injection in light oil reservoirs, in: SPE/PAPG Pakistan Section Annual Technical Conference, Society of Petroleum Engineers, 2015.
- [67] M. Arif, A. Barifcani, M. Lebedev, S. Iglauder, Structural trapping capacity of oil-wet caprock as a function of pressure, temperature and salinity, *Int. J. Greenh. Gas Control* 50 (2016) 112–120.
- [68] H. Al-Mukainah, A. Al-Yaseri, N. Yekeen, J. Al Hamad, M. Mahmoud, Wettability of shale-brine-H₂ system and H₂-brine interfacial tension for assessment of the sealing capacities of shale formations during underground hydrogen storage, *Energy Reports* 8 (2022) 8830–8843.
- [69] S. Iglauder, M. Ali, A. Keshavarz, Hydrogen wettability of sandstone reservoirs: implications for hydrogen geo-storage, *Geophys. Res. Lett.* 48 (3) (2021) 1–5.
- [70] N.K. Jha, A. Al-Yaseri, M. Ghasemi, D. Al-Bayati, M. Lebedev, M. Sarmadivaleh, Pore scale investigation of hydrogen injection in sandstone via X-ray micro-tomography, *Int. J. Hydrol. Energy* 46 (70) (2021) 34822–34829.
- [71] N.K. Jha, M. Lebedev, S. Iglauder, M. Ali, H. Roshan, A. Barifcani, J.S. Sangwai, M. Sarmadivaleh, Pore scale investigation of low salinity surfactant nanofluid injection into oil saturated sandstone via X-ray micro-tomography, *J. Colloid Interface Sci.* 562 (2020) 370–380.
- [72] N. Jha, M. Ali, M. Sarmadivaleh, S. Iglauder, A. Barifcani, M. Lebedev, J. Sangwai, Low salinity surfactant nanofluids for enhanced CO₂ storage application at high pressure and temperature, in: Fifth CO₂ Geological Storage Workshop, European Association of Geoscientists & Engineers, 2018, pp. 1–4.
- [73] N.K. Jha, M. Ali, S. Iglauder, M. Lebedev, H. Roshan, A. Barifcani, J.S. Sangwai, M. Sarmadivaleh, Wettability alteration of quartz surface by low-salinity surfactant nanofluids at high-pressure and high-temperature conditions, *Energy Fuel* 33 (8) (2019) 7062–7068.
- [74] D. Broseta, N. Tonnet, V. Shah, Are rocks still water-wet in the presence of dense CO₂ or H₂? *Geofluids* 12 (4) (2012) 280–294.
- [75] A.S. Al-Menhal, S. Krevor, Capillary trapping of CO₂ in oil reservoirs: observations in a mixed-wet carbonate rock, *Environ. Sci. Technol.* 50 (5) (2016) 2727–2734.
- [76] P. Chiquet, D. Broseta, S. Thibeau, Wettability alteration of caprock minerals by carbon dioxide, *Geofluids* 7 (2) (2007) 112–122.
- [77] T. Rahman, M. Lebedev, A. Barifcani, S. Iglauder, Residual trapping of supercritical CO₂ in oil-wet sandstone, *J. Colloid Interface Sci.* 469 (2016) 63–68.
- [78] S. Iglauder, A. Al-Yaseri, Improving basalt wettability to de-risk CO₂ geo-storage in basaltic formations, *Adv. Geo-Energy Res.* 5 (3) (2021) 347–350.
- [79] M. Ali, M.F. Sahito, N.K. Jha, S. Memon, A. Keshavarz, S. Iglauder, A. Saeedi, M. Sarmadivaleh, Effect of nanofluid on CO₂-wettability reversal of sandstone formation; implications for CO₂ geo-storage, *J. Colloid Interface Sci.* 559 (2020) 304–312.
- [80] A. Abramov, A. Keshavarz, S. Iglauder, Wettability of fully hydroxylated and alkylated (001) α -quartz surface in carbon dioxide atmosphere, *J. Phys. Chem. C* 123 (14) (2019) 9027–9040.
- [81] A. Al-Yaseri, H. Roshan, Y. Zhang, T. Rahman, M. Lebedev, A. Barifcani, S. Iglauder, Effect of the temperature on CO₂/brine/dolomite wettability: hydrophilic versus hydrophobic surfaces, *Energy Fuel* 31 (6) (2017) 6329–6333.
- [82] M. Arif, S. Abu-Khamsin, S. Iglauder, Wettability of rock/CO₂/brine and rock/oil/CO₂-enriched-brine systems: critical parametric analysis and future outlook, *Adv. Colloid Interf. Sci.* 268 (2019) 91–113.
- [83] M. Arif, A.Z. Al-Yaseri, A. Barifcani, M. Lebedev, S. Iglauder, Impact of pressure and temperature on CO₂-brine-mica contact angles and CO₂-brine interfacial tension: implications for carbon geo-sequestration, *J. Colloid Interface Sci.* 462 (2016) 208–215.
- [84] N. Yekeen, E. Padmanabhan, H. Abdulelah, S.A. Irfan, O.A. Okunade, J.A. Khan, B.M. Negash, CO₂/brine interfacial tension and rock wettability at reservoir conditions: a critical review of previous studies and case study of black shale from Malaysian formation, *J. Pet. Sci. Eng.* 196 (2021), 107673.
- [85] M. Hosseini, J. Fahimpour, M. Ali, A. Keshavarz, S. Iglauder, Capillary sealing efficiency analysis of caprocks: implication for hydrogen geological storage, *Energy Fuel* 36 (7) (2022) 4065–4075.
- [86] S. Iglauder, W. Willing, C.H. Pentland, S.K. Al-Mansoori, M.J. Blunt, Capillary-trapping capacity of sandstones and sandpacks, *SPE J.* 16 (04) (2011) 778–783.
- [87] L.P. Daké, Fundamentals of Reservoir Engineering, Elsevier, 1983.
- [88] S. Al Ghafri, G.C. Maitland, J.M. Trusler, Densities of aqueous MgCl₂ (aq), CaCl₂ (aq), KI (aq), NaCl (aq), KCl (aq), AlCl₃ (aq), and (0.964 NaCl + 0.136 KCl)(aq) at temperatures between (283 and 472) K, pressures up to 68.5 MPa, and molalities up to 6 mol·kg⁻¹, *J. Chem. Eng. Data* 57 (4) (2012) 1288–1304.
- [89] O. Kunz, W. Wagner, The GERG-2008 wide-range equation of state for natural gases and other mixtures: an expansion of GERG-2004, *J. Chem. Eng. Data* 57 (11) (2012) 3032–3091.
- [90] J.W. Leachman, R.T. Jacobsen, S. Penoncello, E.W. Lemmon, Fundamental equations of state for parahydrogen, normal hydrogen, and orthohydrogen, *J. Phys. Chem. Ref. Data* 38 (3) (2009) 721–748.
- [91] X. Li, E.S. Boek, G.C. Maitland, J.M. Trusler, Interfacial tension of (brines+ CO₂): (0.864 NaCl + 0.136 KCl) at temperatures between (298 and 448) K, pressures between (2 and 50) MPa, and total molalities of (1 to 5) mol·kg⁻¹, *J. Chem. Eng. Data* 57 (4) (2012) 1078–1088.
- [92] X. Li, E.S. Boek, G.C. Maitland, J.M. Trusler, Interfacial tension of (brines+ CO₂): CaCl₂ (aq), MgCl₂ (aq), and Na₂SO₄ (aq) at temperatures between (343 and 423) K, pressures between (2 and 50) MPa, and molalities of (0.5 to 5) mol·kg⁻¹, *J. Chem. Eng. Data* 57 (5) (2012) 1369–1375.
- [93] M. Bui, C.S. Adjiman, A. Bardow, E.J. Anthony, A. Boston, S. Brown, P.S. Fennell, S. Fuss, A. Galindo, L.A. Hackett, Carbon capture and storage (CCS): the way forward, *Energy Environ. Sci.* 11 (5) (2018) 1062–1176.
- [94] P. Bikkina, J. Wan, Y. Kim, T.J. Kneafsey, T.K. Tokunaga, Influence of wettability and permeability heterogeneity on miscible CO₂ flooding efficiency, *Fuel* 166 (2016) 219–226.
- [95] R. Farokhpour, B.J. Bjørkvik, E. Lindeberg, O. Torsæter, Wettability behaviour of CO₂ at storage conditions, *Int. J. Greenh. Gas Control* 12 (2013) 18–25.
- [96] N.S. Kaveh, A. Barnhoorn, K.-H. Wolf, Wettability evaluation of silty shale caprocks for CO₂ storage, *Int. J. Greenh. Gas Control* 49 (2016) 425–435.
- [97] T.K. Tokunaga, J. Wan, Capillary pressure and mineral wettability influences on reservoir CO₂ capacity, *Rev. Mineral. Geochem.* 77 (1) (2013) 481–503.
- [98] P. Mwangi, P.V. Brady, M. Radonjić, G. Thyne, The effect of organic acids on wettability of sandstone and carbonate rocks, *J. Pet. Sci. Eng.* 165 (2018) 428–435.
- [99] A. Alanazi, M. Ali, M. Mowafi, H. Hoteit, Effect of Organics and Nanofluids on Capillary-sealing Efficiency of Caprock for Hydrogen and Carbon-dioxide Geological Storage, ARMA/DGS/SEG International Geomechanics Symposium, OnePetro, 2022.
- [100] F. Alhamad, M. Ali, M. Ali, H. Abid, H. Hoteit, S. Iglauder, A. Keshavarz, Effect of methyl orange on wettability of sandstone formations: implications for enhanced oil recovery, *Energy Rep.* 8 (2022) 12357–12365.
- [101] M. Aslannezhad, M. Ali, A. Kalantariasl, M. Sayyafzadeh, Z. You, S. Iglauder, A. Keshavarz, A review of hydrogen/rock/brine interaction: implications for hydrogen geo-storage, *Prog. Energy Combust. Sci.* 95 (2023), 101066.
- [102] G.R. Abbasi, M. Arif, A. Isah, M. Ali, M. Mahmoud, H. Hoteit, S. Iglauder, Gas hydrate characterization in sediments via x-ray microcomputed tomography, *Earth Sci. Rev.* (2022), 104233.